

Diffractive color-dipole nucleon scattering

Michael Rueter*, H.G. Dosch

*Institut für Theoretische Physik
Universität Heidelberg
Philosophenweg 16, D-69120 Heidelberg, FRG*

*e-mail: M.Rueter@ThPhys.Uni-Heidelberg.DE
H.G.Dosch@ThPhys.Uni-Heidelberg.DE*

Abstract

We determine the diffractive scattering amplitude of a color-dipole on a nucleon using a non-perturbative model of QCD which contains only parameters taken from low-energy physics. This allows to relate specific features of the confinement mechanisms with diffractive electro-production processes and structure functions. The agreement with phenomenological data is satisfactory.

*supported by the Deutsche Forschungsgemeinschaft

Introduction

In strong interaction physics the infra-red behavior of QCD is relevant both in the low- and high-energy domain. In hadron spectroscopy this is evident, but also in high-energy reactions at small momentum transfer non-perturbative effects play a crucial role. Normally the non-perturbative input in low-energy physics (e.g. intra-quark potentials) and high-energy physics (e.g. structure functions) are conceptually and computationally seen quite separately. In this letter we calculate the high-energy diffractive scattering of color-dipoles on a nucleon in a non-perturbative model of QCD, the parameters of which are fixed only by low-energy input. Our results are compared with other approaches and experimental data.

Since several years one of the authors (H.G.D.) and Yu.A. Simonov have proposed a model in which the non-perturbative features of QCD are approximated by a Gaussian stochastic process which is characterized by the gauge-invariant non-local gluon field-strength correlator [1]-[3]. This correlator is characterized by a correlation length a and its value at zero separation, the gluon condensate $\langle g^2 FF \rangle$. This model of the stochastic vacuum (MSV) yields linear confinement [1] in a very simple and natural way; a nice feature of the model is that confinement only occurs in non-Abelian theories.

The MSV has also been applied to diffractive high-energy scattering [4]-[6], lepto-production of vector-mesons [7] and γ^*p -interaction [8]. Here the natural ingredient (see next section for more details) is the expectation value of two Wegner-Wilson-loops with light-like sides, which correspond to the world-lines of two color-neutral dipoles [9] [10][4]. A characteristic feature of the application of the MSV to diffractive high-energy scattering is the fact that the same mechanism, which is responsible for confinement, leads to a typical dependence of the cross-sections on the loop extensions (dipole sizes): Even if the dipole size is large as compared to the correlation length a of the correlator, the total cross-section still increases with the dipole size. Thus the model implies string-string-interaction and can not lead to quark-additivity. Nevertheless, the ratio of the total cross-sections off nucleon-nucleon- and nucleon-meson-scattering agrees with experiment without additional parameters, this is due to the different radii of the nucleon and mesons, given by the electro-magnetic form-factor [4]. This dependence on the radii also leads to a typical relation between the total cross-section and the logarithmic slope of the elastic cross-section for different hadrons which is in agreement with the experimental data [4].

In this letter we concentrate on the high-energy diffractive scattering of a color-dipole of arbitrary size on a proton. This process is phenomenologically very interesting because it can be used to describe for example the diffractive electro-production of vector-mesons, where due to the photon wave-function (in light-cone perturbation theory [11][12]) dipoles of arbitrary size occur in the interaction. For the proton we use a diquark-picture, which works in all our applications to high-energy scattering better than a three-body-picture. Especially the necessary suppression of the coupling of the odderon to the nucleon is achieved in that way [5][6]. So, the electro-production of vector-mesons can

be build from dipole-dipole-scattering and is illustrated in fig.(1).

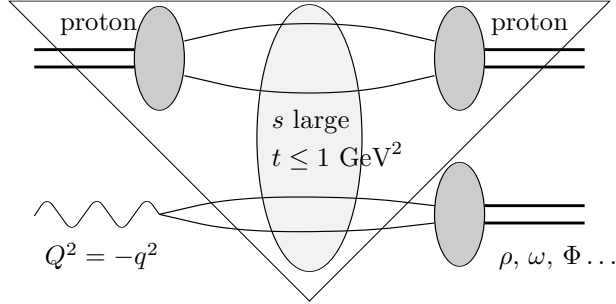


Figure 1: Diffractive electro-production of vector-mesons can be viewed as the diffractive scattering of color-dipoles ($q\bar{q}$ -pair for the photon and q -diquark-pair for the proton) folded with wave-functions. In this letter we calculate only the part inside the triangular, that is the diffractive scattering of the proton on a dipole of arbitrary size.

For large Q^2 the virtual photon (at least the longitudinal polarized one) interacts like a small dipole. In the phenomenological interesting regime dipole sizes between 0.1 fm and 1 fm are most interesting, where the cross-over from perturbative to non-perturbative physics occurs.

Dipole-proton-scattering amplitude

Nachtmann has developed a scheme which allows the separation of the hard high-energy scale from the soft scale of momentum transfer [9]. He considered quark-(anti-)quark-scattering first in an external gluon field in the eikonal approximation. In this way each (anti-)quark picks up the eikonal phase

$$\mathcal{P}e^{-ig \int_C \mathbf{A}_\mu(x) dx^\mu} \quad (1)$$

where the path C is the classical (nearly) light-like path of the (anti-)quark, \mathbf{A}_μ is the matrix-valued color-potential and \mathcal{P} stands for path ordering. The quantum transition amplitudes are obtained by functional integration over the color-field with the QCD-action as exponential weight. In our treatment of high-energy scattering we want to apply the MSV for this integration. We therefore consider not quark-quark-scattering but rather scattering of color-neutral dipoles. In that way we obtain from the eikonal factors (eq.(1)) Wegner-Wilson-loops, i.e. traces of line integrals around closed loops whose light-like sides are the paths of the constituents of the dipole (see fig.(2)). The scattering amplitude of two dipoles with transversal extension \vec{R}_1 and \vec{R}_2 respectively and impact parameter \vec{b} is given by:

$$\tilde{J}(\vec{b}, \vec{R}_1, \vec{R}_2) = - < \frac{1}{N_C} \text{Tr} [\mathbf{W}[\partial S_1] - \mathbf{1}] \cdot \frac{1}{N_C} \text{Tr} [\mathbf{W}[\partial S_2] - \mathbf{1}] >. \quad (2)$$

The brackets ($< \dots >$) denote the functional integration over the gluon-field. In order to perform this integration we first transform the line integrals over \mathbf{A}_μ along the loops $\partial S_1, \partial S_2$ in surface integrals over the field-strengths and

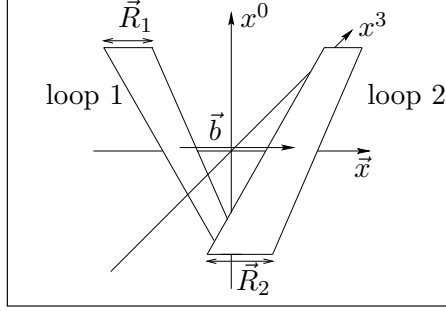


Figure 2: The two W-loops with transversal extension \vec{R}_1 and \vec{R}_2 and light-like sides. Loop 1 describes a color-dipole moving in negative x^3 -direction and loop 2 a color-dipole moving in positive x^3 -direction. The impact parameter \vec{b} is chosen to be purely transversal.

then expand the exponentials. For the resulting functional integration over the field-strengths we use the ansatz of the MSV [1] [4]:

$$\begin{aligned}
& \langle g^2 F_{\mu\nu}^A(z, w) F_{\rho\sigma}^B(0, w) \rangle \\
&= \frac{\delta^{AB}}{N_C^2 - 1} \frac{\langle g^2 FF \rangle}{12} \left\{ \kappa (g_{\mu\rho} g_{\nu\sigma} - g_{\mu\sigma} g_{\nu\rho}) D(z) \right. \\
&\quad \left. + (1 - \kappa) \frac{1}{2} [\partial_\mu (z_\rho g_{\nu\sigma} - z_\sigma g_{\nu\rho}) + \partial_\nu (z_\sigma g_{\mu\rho} - z_\rho g_{\mu\sigma})] D_1(z) \right\}. \quad (3)
\end{aligned}$$

The correlation functions D and D_1 are fitted to lattice results of the non-local correlator [13][14], they fall off on a length scale given by the correlation length a .

In leading order of the expansion of the W-loops we obtain a real scattering amplitude where only transversal coordinates enter. In ref. [4] only the D -function of the non-local correlator was taken into account. Including the D_1 -function we find for eq.(2):

$$\begin{aligned}
\tilde{J} &= \frac{1}{8N_C^2(N_C^2 - 1)144} \tilde{\chi}^2 \\
\tilde{\chi} &= \langle g^2 FF \rangle \left(\kappa \int_0^1 dw_1 \int_0^1 dw_2 \left[\vec{r}_{1q} \cdot \vec{r}_{2q} \mathcal{F}_2[i\tilde{D}] (w_1 \vec{r}_{1q} - w_2 \vec{r}_{2q}) \right. \right. \\
&\quad \left. \left. + \vec{r}_{1\bar{q}} \cdot \vec{r}_{2\bar{q}} \mathcal{F}_2[i\tilde{D}] (w_1 \vec{r}_{1\bar{q}} - w_2 \vec{r}_{2\bar{q}}) \right. \right. \\
&\quad \left. \left. - \vec{r}_{1q} \cdot \vec{r}_{2\bar{q}} \mathcal{F}_2[i\tilde{D}] (w_1 \vec{r}_{1q} - w_2 \vec{r}_{2\bar{q}}) \right. \right. \\
&\quad \left. \left. - \vec{r}_{1\bar{q}} \cdot \vec{r}_{2q} \mathcal{F}_2[i\tilde{D}] (w_1 \vec{r}_{1\bar{q}} - w_2 \vec{r}_{2q}) \right] \right. \\
&\quad \left. + (1 - \kappa) \left[\mathcal{F}_2[i\tilde{D}'_1] (\vec{r}_{1q} - \vec{r}_{2q}) + \mathcal{F}_2[i\tilde{D}'_1] (\vec{r}_{1\bar{q}} - \vec{r}_{2\bar{q}}) \right. \right. \\
&\quad \left. \left. - \mathcal{F}_2[i\tilde{D}'_1] (\vec{r}_{1q} - \vec{r}_{2\bar{q}}) - \mathcal{F}_2[i\tilde{D}'_1] (\vec{r}_{1\bar{q}} - \vec{r}_{2q}) \right] \right). \quad (4)
\end{aligned}$$

The vectors \vec{r} are defined in fig.(3) and \mathcal{F}_2 denotes the two dimensional Fourier-transformed of the correlation functions D and D_1 in the transversal plane.

Using the explicit ansatz given in ref. [4] we have:

$$\begin{aligned}
\mathcal{F}_2[i\tilde{D}(\vec{k})](\vec{x}) &= \int \frac{d^2k}{(2\pi)^2} i\tilde{D}(\vec{k}) e^{i\vec{k}\cdot\vec{x}} \\
&= \frac{\pi}{2} \left[6 \frac{|\vec{x}|^2}{\lambda^2} K_2\left(\frac{|\vec{x}|}{\lambda}\right) - \frac{|\vec{x}|^3}{\lambda^3} K_3\left(\frac{|\vec{x}|}{\lambda}\right) \right] \lambda^2 \\
\mathcal{F}_2[i\tilde{D}'_1(\vec{k})](\vec{x}) &= \pi \frac{|\vec{x}|^3}{\lambda^3} K_3\left(\frac{|\vec{x}|}{\lambda}\right) \lambda^4 \\
\lambda &= \frac{8}{3\pi} a.
\end{aligned} \tag{5}$$

Here K_ν denotes the modified Bessel-functions of second order. One of the w -integrations in eq.(4) can be performed analytically [4].

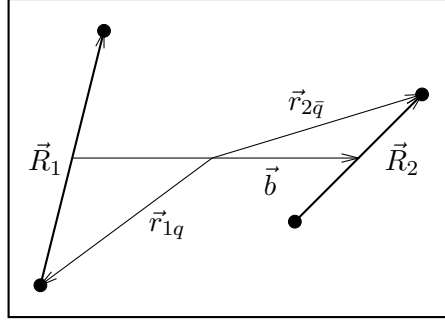


Figure 3: Dipole-dipole-scattering in the transversal plane: \vec{R}_i points from the quark of dipole i to the anti-quark; \vec{b} is the impact parameter and $\vec{r}_{iq(\bar{q})}$ points from the origin to the (anti-)quark of dipole i .

We also include the perturbative interaction which dominates the short distance behavior of the correlation function D_1 . We use the perturbative expression for the non-local correlator in first order with a infra-red cutoff in agreement with the lattice results [14]:

$$\begin{aligned}
&< g^2 F_{\mu\nu}^A(z) F_{\rho\sigma}^B(0) >_{\text{per}} \\
&= \delta^{AB} g^2 \int \frac{d^4k}{(2\pi)^4} e^{-ikz} (-g_{\nu\sigma} k_\mu k_\rho + g_{\nu\rho} k_\mu k_\sigma - g_{\mu\rho} k_\nu k_\sigma + g_{\mu\sigma} k_\nu k_\rho) \tilde{D}'_{\text{per}}(k)
\end{aligned} \tag{6}$$

with

$$\tilde{D}'_{\text{per}}(k) = \frac{i}{k^2 - \frac{1}{c^2}}, \quad c = 0.45 \text{ fm}.$$

For the coupling constant we use here a frozen value of $\alpha_s \approx 0.5$, which is prescribed by our model for consistency reasons [15]-[17]. The perturbative contribution results in an additional term to $\tilde{\chi}$ (eq.(4)):

$$\begin{aligned}
\tilde{\chi}_{\text{per}} &= -\frac{12i}{4} \int_{S_1} \int_{S_2} < g^2 F_{\mu\nu}^A(x, w) F_{\rho\sigma}^A(y, w) >_{\text{per}} d\sigma^{\mu\nu}(x) d\sigma^{\rho\sigma}(y) \\
&= 12(N_C^2 - 1)g^2 [\Delta(\vec{r}_{1q} - \vec{r}_{2q}) + \Delta(\vec{r}_{1\bar{q}} - \vec{r}_{2\bar{q}}) - \\
&\quad \Delta(\vec{r}_{1q} - \vec{r}_{2\bar{q}}) - \Delta(\vec{r}_{1\bar{q}} - \vec{r}_{2q})]
\end{aligned} \tag{7}$$

with

$$\Delta(\vec{x}) = \mathcal{F}_2 \left[\frac{1}{\vec{k}^2 + \frac{1}{c^2}} \right] (\vec{x}) = \frac{1}{2\pi} K_0 \left[\frac{|\vec{x}|}{c} \right]. \quad (8)$$

Because the function $\tilde{\chi}$ enters quadratically in the scattering amplitude (see eq.(4)) we have in addition to the purely perturbative and non-perturbative contribution also an interference term.

In order to come from dipole-dipole- to dipole-hadron-scattering we smear the scattering amplitude (eq.(2)) with a transversal proton wave-function with extension parameter S_p and keep one extension fixed to the dipole size R_D :

$$\hat{J}(\vec{b}, R_D, S_p) = \int \frac{d\varphi_D}{2\pi} \int d^2 R_2 \tilde{J}(\vec{b}, \vec{R}_D, \vec{R}_2) |\Psi(\vec{R}_2, S_p)|^2. \quad (9)$$

The scattering amplitude at center of mass energy s and momentum transfer $t = -\vec{q}^2$ is given by:

$$T(s, t) = 2is \int d^2 b e^{-i\vec{q}\vec{b}} \hat{J}(\vec{b}, R_D, S_p). \quad (10)$$

For the proton (working in the diquark-picture [5] [6]) we use as wave-function:

$$|\Psi(\vec{R}_2, S_p)|^2 = \frac{1}{2\pi} \frac{1}{S_p^2} e^{-\frac{|\vec{R}_2|^2}{2S_p^2}}. \quad (11)$$

For the total cross-section follows:

$$\sigma^{\text{tot}} = \frac{1}{s} \text{Im} T(s, 0) = 2 \int d^2 b \text{Re} [\hat{J}(\vec{b}, R_D, S_p)], \quad (12)$$

which in our model is independent of the center of mass energy s .

Numerical results and comparison with other approaches and experimental data

Nikolaev and Zakharov developed a picture of dipole-nucleon scattering [18]-[21] which is in some respect very similar to the one discussed above. But whereas our main emphasis lies on the calculation of the scattering amplitude $\hat{J}(\vec{b}, R_D, S_p)$ (eq.(9)) they are more interested in the consequences of the dipole-scattering picture especially in the energy dependence due to perturbative QCD. In a recent analysis Nemchik et al. extracted from electro-production data the dipole-proton cross-section $\sigma^{\text{tot}}(s, R_{D1})$ [22][23]. They used the fact that due to the overlap of the wave-functions of the photon with virtuality Q^2 and the produced vector-meson of mass M_V the dipole-nucleon cross-section is mainly probed at the so called scanning radius [24]

$$r_s \approx \frac{6}{\sqrt{Q^2 + M_V^2}}.$$

The results of there analysis of different experiments are shown in fig.(4). There are two distinct domains of energy of the $\gamma^* - p$ -system: The fixed target experiments of the EMC, NMC, E687 and FNAL groups are at the center of

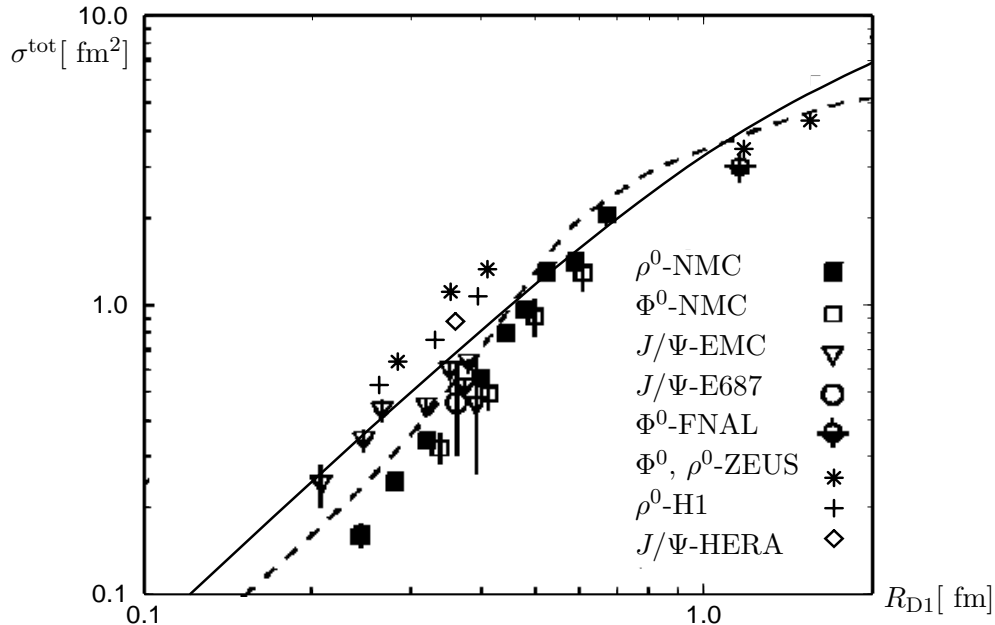


Figure 4: Comparison of our result for the total cross-section for dipole (extension R_{D1}) proton scattering with values extracted from cross-sections of lepto-production of vector-mesons by the method of Nemchik et al. [22][23]. The solid line is our result without any fitting of the parameters to high-energy data. The dashed line is the ansatz of Nemchik et al. for the total cross-section for the fixed target experiments.

mass energy about $W \approx 10 - 15$ GeV, whereas the HERA experiments are at $W \approx 70 - 150$ GeV. The high-energy results are indeed systematically higher than the fixed target results but here we do not discuss this point which is off course of great interest for itself.

The solid line in fig.(4) is our prediction for the dipole-proton cross-section where only low-energy input has been used: the correlator (eq.(3)) taken from the lattice calculations (compatible with the string tension of heavy quarkonia) and the electro-magnetic proton radius ($R^{\text{em}} = 0.862$ fm [25]). We see that the agreement with the extracted phenomenological points is satisfactory and encourages the approach to relate high- and low-energy data.

Of special interest is the agreement of our calculation at values of R_{D1} larger than the correlation length $a \approx 0.3$ fm. If quark-additivity would hold the dipole cross-section should level off around that value of R_{D1} . The continued increase shows that the most specific feature of non-perturbative QCD, namely confinement, leaves its traces also in high-energy scattering.

Acknowledgments

The authors want to thank A. Hebecker, O. Nachtmann and H.J. Pirner for discussions. M.R. thanks the Deutsche Forschungsgemeinschaft for financial support.

References

- [1] H.G. Dosch, *Phys.Lett.* **B190** (1987) 177.
- [2] H.G. Dosch and Y.A. Simonov, *Phys.Lett.* **B205** (1988) 339.
- [3] Y.A. Simonov, *Nucl.Phys.* **B307** (1988) 512.
- [4] H.G. Dosch, E. Ferreira and A. Krämer, *Phys.Rev.* **D50** (1994) 1992.
- [5] M. Rueter and H.G. Dosch, *Phys.Lett.* **B380** (1996) 177.
- [6] M. Rueter, Proceedings of the workshop “*Diquarks III*”, Torino, hep-ph-9612338 (1996).
- [7] H.G. Dosch, T. Gousset, G. Kulzinger and H.J. Pirner, *Phys.Rev.* **D55** (1997) 2602.
- [8] H.G. Dosch, T. Gousset and H.J. Pirner, hep-ph-9707264 (1997).
- [9] O. Nachtmann, *Annals Phys.* **209** (1991) 436.
- [10] O. Nachtmann, Lectures, Schladming (Austria), hep-ph-9609365 (1996).
- [11] J.D. Bjorken, J.B. Kogut and D.E. Soper, *Phys.Rev.* **D3** (1971) 1382.
- [12] G.P. Lepage and S.J. Brodsky, *Phys.Rev.* **D22** (1980) 2157.
- [13] A. Di Giacomo and H. Panagopoulos, *Phys.Lett.* **B285** (1992) 133.
- [14] A. Di Giacomo, E. Meggiolaro and H. Panagopoulos, hep-lat-9603017 (1996).
- [15] M. Rueter and H.G. Dosch, *Z.Phys.* **C66** (1995) 245.
- [16] H.G. Dosch, O. Nachtmann and M. Rueter, hep-ph-9503386 (1995).
- [17] M. Rueter, Proceedings of the conference “*Quark Confinement and the Hadron Spectrum II*”, Como, hep-ph-9610215 (1996).
- [18] N.N. Nikolaev and B.G. Zakharov, *Z.Phys.* **C49** (1991) 607.
- [19] N.N. Nikolaev and B.G. Zakharov, *Z.Phys.* **C53** (1992) 331.
- [20] N.N. Nikolaev and B.G. Zakharov, *Z.Phys.* **C64** (1994) 631.
- [21] N.N. Nikolaev and B.G. Zakharov, *Phys.Lett.* **B327** (1994) 149.
- [22] J. Nemchik, N.N. Nikolaev, E. Predazzi and B.G. Zakharov, *Phys.Lett.* **B374** (1996) 199.
- [23] J. Nemchik, N.N. Nikolaev, E. Predazzi and B.G. Zakharov, hep-ph-9605231 (1996).
- [24] J. Nemchik, N.N. Nikolaev and B.G. Zakharov, *Phys.Lett.* **B341** (1994) 228.
- [25] G.G. Simon et al., *Z. Naturforsch.* **A35** (1980) 1.